

**CONTACT ANGLE OF WATER ON IRON ORE FINES:  
MEASUREMENT AND ANALYSIS****X.B. Huang<sup>a</sup>, X.W. Lv<sup>a,\*</sup>, J.J. Song<sup>B</sup>, C.G. Bai<sup>a</sup>, R.D. Zhang<sup>a</sup>, M.J. Zhou<sup>C</sup>**<sup>a</sup> College of Materials Science and Engineering, Chongqing University, Chongqing, China<sup>b</sup> Center of Material for Chongqing Metrology Institute of Quality Inspection, Chongqing, China<sup>c</sup> Ironmaking plant, Baoshan Iron & Steel Co., Ltd., Shanghai, China.*(Received 03 September 2014; accepted 08 November 2014)***Abstract**

The relative contact angle ( $\theta_{RC_A}$ ) for seven iron ore fines was measured by using Washburn Osmotic Pressure method under laboratory conditions. By choosing cyclohexane as the reference that can perfectly wet iron ore particles, the relative contact angles were measured and varied from 57° to 73°. With the volume % of goethite ( $\phi_G$ ) as the variable, a new model for relative contact angle was developed. The expected relative contact angle for pure goethite is about 56°, while that for goethite free samples is about 77°. Physical properties, such as surface morphology (SMI) and pore volume ( $V_{pore}$ ) can influence the relative contact angle. The  $\phi_G$  can be expressed as a function of SMI and  $V_{pore}$ . Thus, we inferred that the relative contact angle is a function of  $\phi_G$  for the iron ores used.

The measured relative contact angles were found to be in good agreement ( $R_{adj}^2 > 0.97$ ) with the calculated ones based on the research from Iveson, et al. (2004). Comparing with the model developed by Iveson et al. (2004), the new model for contact angle proposed in this paper is similar, but more detailed with two meaningful physical parameters.

The modification of physicochemical properties on iron ores would be another topic in the further study on granulation.

**Keywords:** Wettability; Washburn osmotic pressure method; Relative contact angle; Physicochemical properties

**1. Introduction**

As one of the solid-liquid interfacial properties, contact angle ( $\theta$ ) is widely studied and used in flotation, wet grinding, decontamination, lubrication, cleaning, coating and painting, etc. [1, 2]. In iron ore sintering, the final granule strength and the optimal moisture content in granulation are largely determined by the water contact angle of the iron ores [3-5]. As reported [4, 6], the influence of wettability ( $\cos(\theta)$ ) on the granulation of porous materials is uncertain. It depends on the net effect of two aspects caused by wettability, the granule strength and the amount of water absorbed at the surface. According to the prediction on tensile strength of granules proposed by Rumpf [6], the granule strength can be enhanced and the amount of water needed in granulation would be reduced by increasing the wettability of the materials. However, the pore saturation of the particles filled by water is proportional to  $\cos(\theta)$ , which indicates that the amount of water would soak more into the pores at lower contact angle. To enhance granule strength and minimize the amount of water used in granulation, there might be a non-zero contact angle of iron ores for a better granulation result [4]. The

contact angle for seven iron ore fines was determined and its influence factors were analysed in this paper.

In all techniques of contact angle measurement, capillary rise methods are widely adopted in the measurement of advancing contact angle ( $\theta_a$ ) on real material surfaces [4, 7-9]. More specifically, according to the capillary flow of a fluid in packed bed, Washburn penetration methods were proposed [10] and developed [1, 4, 9] to measure the contact angle of powders. In this work, Washburn osmotic pressure method [11, 12] was adopted in the measurement of contact angle for seven iron ore fines. In practice, it is problematic to determine the structure-related parameters in Washburn equation [8, 10] directly. Thus the relative water contact angle was proposed and determined by using cyclohexane as the perfectly wetting liquid (the reference liquid) in the measurement on iron ore fines [8].

Finally, the effect of some physicochemical properties on relative contact angle of iron ore fines was studied and discussed. The results in this paper may extend our understanding of the conclusions drawn by Simon M. Iveson, et al. [1, 4]. Besides, some potential methods to enhance granulation of a sinter mixture were also discussed.

\* Corresponding author: lvxuewei@163.com

## 2. Theory and Method

### 2.1 Contact Angle and Capillary flow

In non-reactive systems [2] or where the reactions between different phases can be negligible, the contact angle ( $\theta$ ) on an ideal surface is defined by the well-known Young equation [13]:

$$\sigma_{l-v} \cos \theta = \sigma_{s-v} - \sigma_{s-l} \quad (1)$$

Where,  $\sigma_{l-v}$ ,  $\sigma_{s-v}$  and  $\sigma_{s-l}$  are the surface tensions (N/m or J/m<sup>2</sup>) of liquid-vapour, solid-vapour and solid-liquid, respectively. And,  $\cos(\theta)$  is the cosine of contact angle ( $\theta$ , °), which is the angle [14] between the liquid-vapour surface and the liquid-solid surface along the three phase contact lines. According to the dynamic behaviour of the interactions between a solid surface and a liquid, two categories of contact angles are classified, viz., an advancing contact angle ( $\theta_A$ ) for a liquid advancing across the surface and a receding angle ( $\theta_R$ ) for the liquid receding from the surface [15]. This paper researched a process where the water flows into a packed bed of iron ore particles driven by capillary forces, thus only advancing contact angle need to be concerned.

Dynamic capillary rise techniques are the methods mainly used for determining the contact angle of a powder [7], which were popularized by Washburn (1921) [10], validated by Fisher and Lark (1979) [16] and developed theoretically by Good and Lin (1976) [17] and Levine et al. (1980) [18]. In capillary driven flow, the capillary driving force ( $\Delta P_{cap}$ ) generated by a fluid in capillary tubes is given by the Young Laplace equation [19]. The viscous resistance ( $\Delta P_{vis}$ ) when a fluid flow in capillary tubes is described by the Hagen–Poiseuille equation [20]. Neglecting inertial and gravity effects, combining the viscous resistance ( $\Delta P_{vis}$ ) and the capillary driving force ( $\Delta P_{cap}$ ) yields the rate of liquid penetration ( $u=dh/dt$ ) for the fluid flowing in capillary tubes [10].

$$u = \frac{dh}{dt} = \frac{R_D \sigma_{l-v} \cos \theta_A}{4h\eta} \quad (2)$$

Where,  $R_D$  is the mean hydrodynamic radius of capillary tubes in a packed bed (m);  $u$ ,  $\eta$  and  $h$  are the velocity (m/s), viscosity (Pa.s) and penetration height (m) after  $t$  seconds of penetration, respectively.  $\theta_A$  and  $\sigma_{l-v}$  are referred as the mentioned advancing contact angle and the surface tension of the testing liquid.

The penetration for a liquid flowing into capillary tubes in a cylinder sealed at one end can be described by a two-stage mechanism [21]. Initially, capillary driven flow will continue penetrating until the pressure of the trapped air in the cylinder balances the capillary pressure generated in these tubes. Then, a gradual decrease in the volume of the trapped air will occur due to the air dissolution. This process will take a long time (more than an hour [21]), which means the water absorbed by air dissolution plays little role in

iron ore granulation. Thus the influence of air dissolution can be ignored in this study. The first stage of the liquid penetration is described by equation (2) and it is the process where the relative contact angle of the iron ore fines was measured.

### 2.2 Washburn Osmotic Pressure Method

Integrating equation (2) yields the well-known Lucas–Washburn equation [10, 16, 22, 23], which is given as below:

$$h^2 = \frac{R_D \sigma_{l-v} \cos \theta_A}{2\eta} t \quad (3)$$

When using equation (3) to measure the contact angle of a powder, some problems have been encountered [11, 24]. One of the problems is that the accurate height of the liquid front is difficult to acquire. However, with high accurate pressure sensors been developed and widely used in industrial and academic fields, it is easily to measure the contact angle of a powder in a packed bed by using the Washburn Osmotic Pressure method [1, 11, 12, 24].

Some assumptions to generate Washburn Osmotic Pressure equation from the Lucas–Washburn equation (equation (3)) were adopted. Firstly, for a capillary flow in a packed bed, the porous structure in the packed bed is homogenous and stable with an effective cross-sectional area of  $A$ . And, the pressure increment ( $\Delta P$ ) under a penetration height of  $h$  after  $t$  seconds of penetration is much less than the initial pressure of the inner air ( $P_0$ ). Taking the inner air (an initial volume of  $V_0$ ) as the research object with the ideal gas properties applied to the air, the relationship between the pressure increment ( $\Delta P$ ) and the penetration height ( $h$ ) can be found in equation (4).

$$h = \frac{V_0}{P_0 * A} \Delta P \quad (4)$$

Where,  $h$  is the penetration height after  $t$  seconds of penetration in the packed bed;  $V_0$  is the initial volume (m<sup>3</sup>) of the inner air in the testing tube;  $P_0$  is the initial pressure (Pa) of the inner air and  $\Delta P$  is the pressure increment (Pa) of the inner air after  $t$  seconds of liquid penetration;  $A$  is the effective cross-sectional area (m<sup>2</sup>) of the packed bed in the testing system.

Substituting  $h$  from equation (4) into equation (3), the Washburn osmotic pressure method to measure contact angle of iron ore fines is given by equation (5).

$$(\Delta P)^2 = \frac{\beta \sigma_{l-v} \cos \theta_A}{2\eta} t \quad (5)$$

Where,  $\beta$  is a structure-related parameter (N<sup>2</sup>.m<sup>-5</sup>), which is determined by the packed status ( $R_D$ ,  $A$  and  $V_0$ ) and the initial air pressure  $P_0$ . This parameter ( $\beta$ ) is usually treated as a constant in batches of measurements with the same sample. But the value of  $\beta$  is difficult to obtain, which makes difficult to

calculate the value of contact angle with equation (5).

To avoid calculating  $\beta$  directly, cyclohexane with a surface tension less than 0.030 N/m was adopted as the reference liquid in the contact angle measurements of iron ore fines [1, 8]. Here, cyclohexane can perfectly wet the surface of the iron ore particles ( $\cos(\theta_{\text{cyclohexane}}) = 1$ ). Thus, the relative contact angle ( $\theta_{\text{RCA}}$ ) of water on iron ore fines can be calculated by equation (6).

$$\cos(\theta_{\text{RCA}}) = \frac{k\eta/\sigma_{\text{L-V}}}{k_0\eta_0/\sigma_{\text{L-V}0}} \quad (6)$$

Where,  $k$  or  $k_0$  is the slope of the  $(\Delta P)^2 - t$  curve described by equation (5).  $k_0$ ,  $\eta_0$  and  $\sigma_{\text{L-V}0}$  are the parameters with cyclohexane as the testing liquid; while  $k$ ,  $\eta$  and  $\sigma_{\text{L-V}}$  are the parameters when water is used. In practice, we calculated  $k$  in a linear curve ( $R_{\text{adj}}^2 > 0.98$ ) from the  $(\Delta P)^2 - t$  curve in a period of penetration time from  $t$  to  $t + \Delta t$  ( $t > 0$  s,  $\Delta t > 120$  s).

### 3. Apparatus and Materials

Developed based on the mentioned Washburn Osmotic Pressure equation (equation (5)), a commercial apparatus, JF99A made by Shanghai Zhongchen Digital Technic Apparatus Co., LTD was adopted in the contact angle measurements for seven commercial iron ore fines. The schematic of JF99A was shown in Figure 1.

The true density ( $\rho_{\text{ore}}$ ) of iron ores was measured by volumetric displacement of water in a 250 ml flask. The chemical composition and true density for the seven iron ore fines were shown in Table 1. According to the definition of LOI (loss on ignition), we suppose that the decomposition of goethite ( $\text{Fe}_2\text{O}_3 \cdot \text{H}_2\text{O}$ ) contributes a great to the value of LOI for the iron ores

used. Thus the iron ores used here have three kinds of iron oxides: magnetite ( $\text{Fe}_3\text{O}_{4\text{M}}$ ), free hematite ( $\text{Fe}_2\text{O}_{3\text{FH}}$ ) and goethite ( $\text{Fe}_2\text{O}_3 \cdot \text{H}_2\text{O}_{\text{G}}$ ). The content of those iron oxides in iron ores used will be calculated and discussed later in this paper.

**Table 1.** Chemical composition (mass %) and density ( $10^3 \cdot \text{kg/m}^3$ ) for iron ores used

Sample	TFe	FeO	CaO	SiO <sub>2</sub>	Al <sub>2</sub> O <sub>3</sub>	MgO	LOI	$\rho_{\text{ore}}$
S1	61.53	0.29	0.02	3.05	2.06	0.16	6.34	4.32
S2	63.34	0.71	0.05	5.74	1.12	0.05	2.19	4.9
S3	64.51	0.45	0.02	4.3	0.68	0.05	2.04	4.96
S4	58.27	0.22	0.04	5.55	1.37	0.08	10.13	3.93
S5	59.14	0.21	0.05	4.38	1.5	0.08	9.52	4.08
S6	61.26	0.32	0.03	3.69	2.25	0.06	5.88	4.58
S7	65.29	0.16	0.02	1.36	1.49	0.09	2.18	4.49

Some physical properties of the iron ores were measured by nitrogen adsorption technique (ASAP 2020) and laser diffraction method (Mastersizer 2000). The results were shown in Table 2. The specific surface area ( $S_{\text{BET}}$ ) measured by nitrogen adsorption method represents the specific area of the internal and external surfaces. With the hypothesis that all particles are perfectly spherical, laser diffraction method only can calculate the external surface area ( $S_{\text{LPSA}}$ ) of the particles. In Table 2, there is a big difference between the two surface areas, which can be attributed to the difference of measuring principle on surface area between the two methods.

The difference between the two surface areas may describe the surface morphology of the particles. In

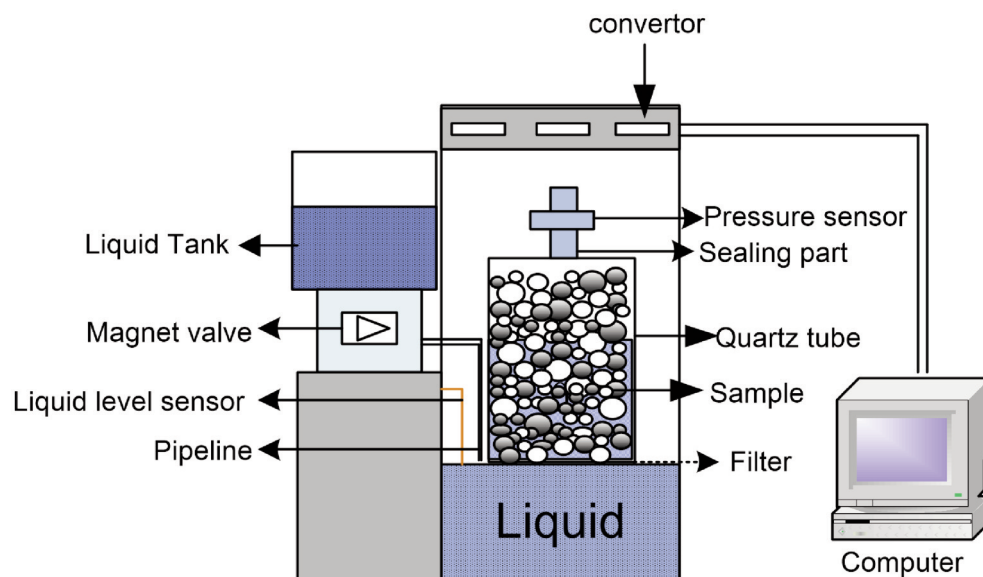


**Figure 1.** Apparatus of contact angle measurement for iron ore fines used

Table 2. Physical properties of iron ores

Sample	S1	S2	S3	S4	S5	S6	S7
$S_{BET}^a (10^3 \cdot m^2/kg)$	9.098	2.888	1.602	24.544	23.462	7.788	6.836
$S_{LPSA}^b (10^3 \cdot m^2/kg)$	0.381	0.174	0.18	0.211	0.396	0.347	0.508
SMI ( $S_{BET} / S_{LPSA}$ )	23.88	16.59	8.9	116.32	59.25	22.44	13.46
$V_{pore}^a (10^{-5} \cdot m^3/kg)$	4.44	0.81	0.61	4.99	4.82	3.6	1.72

<sup>a</sup>-result measured by ASAP 2020,  $V_{pore}$  is the pore volume; <sup>b</sup>- result measured by Mastersizer 2000 ;  $S_{BET}$  is the specific surface area based on BET model;  $S_{LPSA}$  is the specific surface area from laser diffraction method.

consideration of our previous work [25], the ratio of  $S_{BET}$  to  $S_{LPSA}$  was defined as the surface morphology index (SMI) with its value for the seven ores shown in Table 2. To graphically describe the difference in surface morphology, SEM images of these particles were obtained with two typical images for two ores shown in Figure 2. In Figure 2, S4 and S3 are the materials with the roughest and smoothest surface among the seven ores, respectively. From the two images and the value of SMI in Table 2, it seems that the roughness of the ores increases with increasing the value of SMI. According to SMI, the roughness of the ores increases in an order of S3, S7, S2, S6, S1, S5 and S4.

that for cyclohexane are  $0.908 \cdot 10^{-3}$  Pa.s and  $0.025$  N/m, respectively. Substituting the corresponding  $k$ ,  $\eta$  and  $\sigma$  into equation (6), the relative contact angle for each ore was calculated and the results were listed in Table 3. The relative contact angle for these ores varied from  $57^\circ$  to  $73^\circ$ . According to the relative contact angle, the wettability of the ores increases in an order of S3, S2, S7, S6, S1, S5 and S4. This order

4. Results and Discussion

4.1 Relative contact angle for iron ore fines

The typical dynamic osmotic pressure curves  $((\Delta P)^2$  versus  $t$ ) were shown in Figure 3 by using water and cyclohexane as the testing liquid.

These curves were fitted to the equation (5) to calculate the slope ( $k$ ). Under testing temperature (about  $25^\circ C$ ), the viscosity ( $\eta$ ) and surface tension ( $\sigma$ ) for water are  $0.893 \cdot 10^{-3}$  Pa.s and  $0.072$  N/m; while

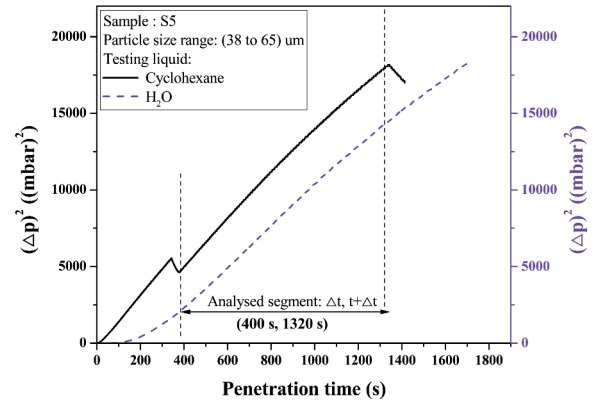
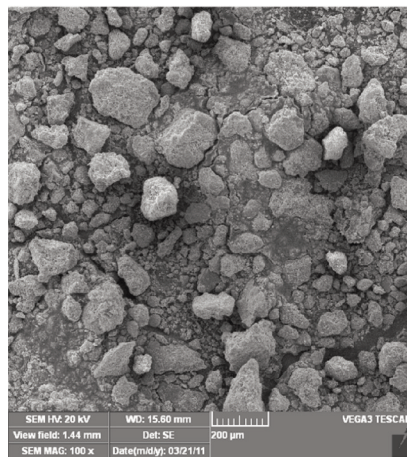
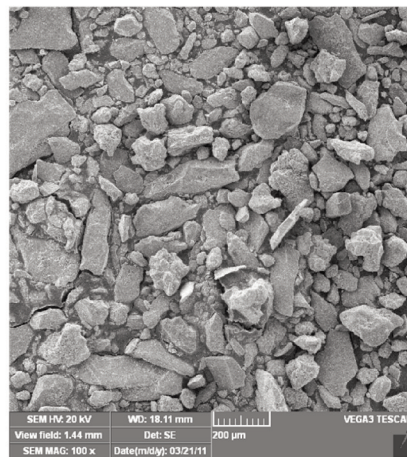


Figure 3. Typical curves of  $(\Delta P)^2$  versus  $t$  for S5 (time span: 400 s to 1320 s)



S4



S3

Figure 2. The SEM images for the surface morphology of S3 and S4

of wettability is quite similar to that of roughness (SMI) and pore volume of the iron ores used.

**Table 3.** Relative contact angle ( $\theta_{RCA}$  and  $\cos(\theta_{RCA})$ ) for the iron ores used

Samples	S1	S2	S3	S4	S5	S6	S7
$\cos(\theta_{RCA})$	0.45	0.32	0.29	0.55	0.51	0.4	0.39
$\theta_{RCA}$ (°)	63	71	73	57	59	66	67

#### 4.2 A new model for relative contact angle

As mentioned in ‘‘Apparatus and Materials’’, the majority of LOI comes from the decomposition of goethite ( $Fe_2O_3 \cdot H_2O_G$ ), while the decomposition of other hydroxides (such as kaolinite ( $Al_2Si_2O_5(OH)_4$ )), the degasification ( $CO_2$  and  $SO_2$ ) and other reactions contribute a little to the value of LOI. Here we define  $LOI^0$  as the minority of LOI that comes from other reactions rather than the decomposition of goethite. Then the mass % of goethite in an iron ore can be calculated as follows.

$$Fe_2O_3 * H_2O_G = (LOI - LOI^0) \times \frac{177.72}{18.02} \quad (7)$$

And the magnetite ( $Fe_3O_{4M}$ ), total hematite ( $Fe_2O_{3T}$ ) and free hematite ( $Fe_2O_{3FH}$ ) of the iron ores used can be calculated.

$$Fe_3O_{4M} = FeO \times \frac{231.55}{71.85} \quad (8)$$

$$Fe_2O_{3T} = \left( TFe - FeO \times \frac{167.55}{71.85} \right) \times \frac{159.70}{111.70} \quad (9)$$

$$Fe_2O_{3FH} = Fe_2O_{3T} - Fe_2O_3 * H_2O_G \times \frac{159.70}{177.72} \quad (10)$$

To determine the value of the mass % of goethite and that of free hematite, a proper value of  $LOI^0$  must be given in advance. We suppose that there is a fixed ratio of  $LOI^0$  to LOI and with this  $LOI^0$ , the content of free hematite in an iron ore with the highest LOI has a positive value close to zero. Sample S4 (the highest LOI with the lowest free hematite) was used to determine  $LOI^0$ . The relation of  $LOI^0 = 0.1 \times LOI$  was applied for each ore used in this paper. Thus those iron oxides can be calculated and the result was shown in Table 4.

**Table 4.** Calculation of three iron oxides from chemical composition

Item (mass %)	S1	S2	S3	S4	S5	S6	S7
$LOI^0$	0.63	0.22	0.2	1.01	0.95	0.59	0.22
$Fe_3O_{4M}$	0.93	2.29	1.45	0.71	0.68	1.03	0.52
$Fe_2O_{3T}$	87	88.19	90.73	82.58	83.85	86.52	92.81
$Fe_2O_3 * H_2O_G$	56.27	19.44	18.11	89.92	84.5	52.19	19.35
$Fe_2O_{3FH}$	36.44	70.72	74.46	1.78	7.92	39.62	75.43

The relationship between measured density and calculated goethite content is shown in Figure 4. The density [26] for pure hematite and pure goethite is  $5.24 \times 10^3$  and  $4.3 \times 10^3$  kg/m<sup>3</sup>, respectively. The data of S7 was not used to fit the equation. From the fitted equation in this figure, the density of goethite is about  $3.83 \times 10^3$  kg/m<sup>3</sup>, which is a reasonable value considering that some lower density components and a few closed pores also exist in iron ore particles.

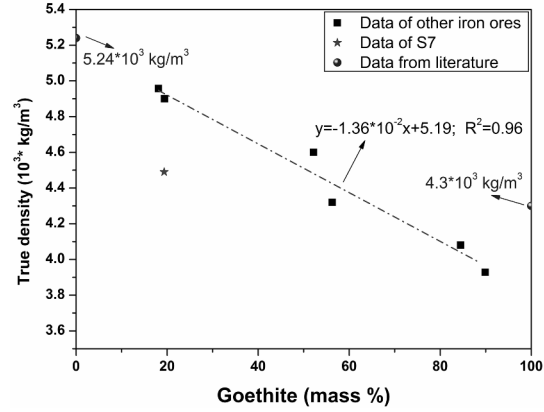


**Figure 4.** Measured density as function of calculated goethite content

Then the volume % of goethite ( $\varphi_G$ ) in an iron ore can be calculated as:

$$\varphi_G = \frac{Fe_2O_3 * H_2O_G}{3.83} \times \rho_{ore} \quad (11)$$

Using the Young-Dupre equation [27], the adhesion energy ( $W$ , J/m<sup>2</sup>) can be calculated as  $\sigma_{l-v} \times (1 + \cos(\theta))$  with the contact angle of water on iron ore fines. Meanwhile, similar to the calculation of viscous Gibbs free energy for mixing [28], by using the rule for average adhesion energy of heterogenous surfaces [29], the adhesion energy between water and the iron ore surfaces can be estimated as:

$$W = W_o \times (1 - \varphi_G) + W_G \times \varphi_G \quad (12)$$

Where,  $W_o$  represents all adhesion energy between water and all non-hydroxide oxides (J/m<sup>2</sup>);  $W_G$  is the adhesion energy between water and goethite (J/m<sup>2</sup>).

Thus, a mathematical model for contact angle with the volume % of goethite ( $\varphi_G$ ) can be built as follows.

$$\sigma_{l-v} \times (1 + \cos(\theta)) = W_o + (W_G - W_o) \times \varphi_G \quad (13)$$

Where,  $\sigma_{l-v}$  is the surface tension of water (0.072 J/m<sup>2</sup>). By drawing  $\sigma_{l-v} \times (1 + \cos(\theta_{RCA}))$  versus  $\varphi_G$  in Figure 5, the model in equation (13) shows good agreement with the experimental data (data of S7 was excluded). This model can be explained by the report [4] that any surface that has a reduced ability of favourable H-bonding interactions with water, would lead to the increase in contact angle of water on the surface.

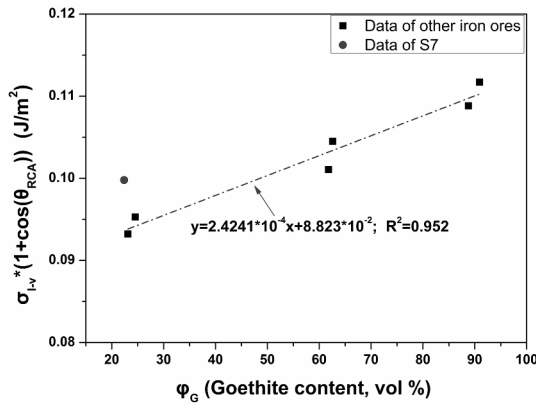


Figure 5. Adhesion energy as function of volume % of goethite for iron ores used.

From Figure 5, the adhesion energy  $W_O$  is  $0.088 \text{ J/m}^2$  and  $W_G$  is  $0.112 \text{ J/m}^2$ . Thus the expected relative contact angle for pure goethite is about 56 degree and that for goethite-free iron ore samples is about 77 degree.

It is reported that both chemical properties [1, 4, 8] and physical properties [30], such as surface roughness and pore distribution, have a significant impact on the wettability of iron ore powders. The impact of physical properties on relative contact angle was described in Figure 6. Given by equation (14) with a correlation coefficient  $R_{adj}^2 = 0.9$  and  $SMI \geq 1$ , an increase in SMI of the iron ores leads to a decrease in the measured relative contact angle.

$$\theta_{RCA} = 90 / SMI^{0.1} \quad (14)$$

This result can be accounted for by knowing that particles with a rough and irregular shape has a bigger value of SMI and are easy to be wetted and granulated [31, 32]. Furthermore, a higher pore volume leads to a lower contact angle, which means that porous

particles favour the wettability between the iron ores and water. As mentioned in “4.1 Relative contact angle of iron ore fines”, there might be a strong relation of the volume % of goethite ( $\phi_G$ ) to surface morphology index (SMI) and pore volume ( $V_{Pore}$ ) of the iron ores studied. By using multilinear regression method, the volume % of goethite ( $\phi_G$ ) can be expressed as a function of SMI and  $V_{Pore}$  with a regression correlation  $R_{adj}^2 = 0.927$ .

$$\phi_G = 0.266 * SMI + 0.769 * V_{Pore} \quad (15)$$

Then taking equation (15) into account, we can infer that the relative contact angle is a function of the volume % of goethite ( $\phi_G$ ). This function can be expressed as a mathematical model given by equation (13).

### 4.3 Comparison with the literature from Iveson et al.

The contact angle measurement conducted by Simon M. Iveson, et al. [4] is based on the capillary pressure difference ( $\Delta P_{cap}$ ) generated by a fluid in a packed bed, which was given by Young-Laplace equation. Due to the difficulty to directly determine the effective mean pore radius ( $r_{eff}$ ) in the Young-Laplace equation. They used a perfectly wetting fluid on iron ore powders to overcome this problem. Their relative contact angle can be determined as:

$$\cos(\theta) = \frac{\sigma_{l-v0} \times \Delta P_{cap}}{\sigma_{l-v} \times \Delta P_{Cap-0}} \quad (16)$$

Where,  $\sigma_{l-v0}$  and  $\Delta P_{cap-0}$  are the surface tension and capillary pressure difference generated by the perfectly wetting liquid in the packed bed;  $\sigma_{l-v}$  and  $\Delta P_{cap}$  are that when water was used in test. In their research work, the capillary pressure difference ( $\Delta P_{cap}$ ) is determined by subtracting hydrostatic pressure ( $\Delta P_{hyd}$ ) from the equilibrium value of the

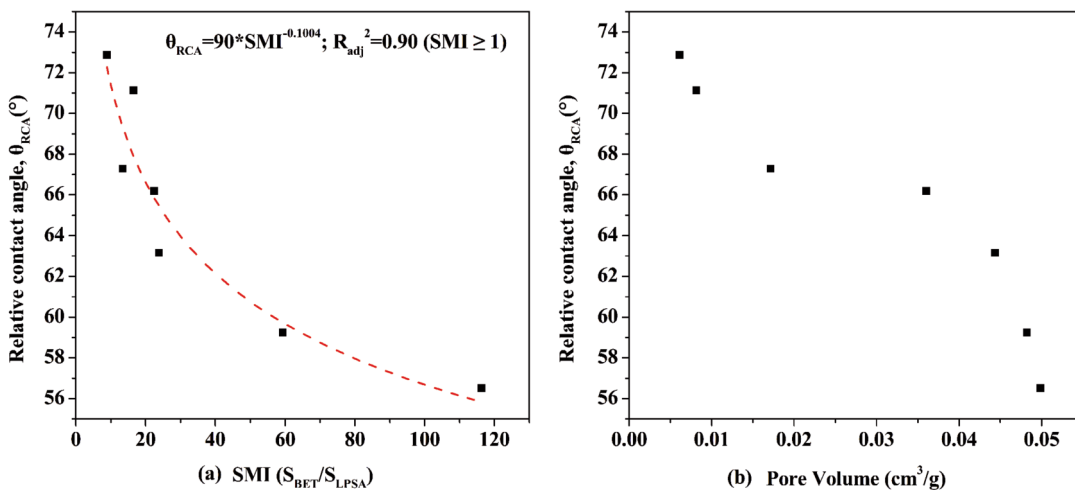


Figure 6. Influence of physical properties on relative contact angle ( $\theta_{RCA}$ ) of iron ores used

changing pressure in the gas space ( $\Delta P_{air}$ ).

According to their research [1, 4], a linear relationship ( $R^2=0.88$ ) between the true density and the hematite content ( $\text{Fe}_2\text{O}_{3H}$ , vol %) of iron ores can be found. And, the measured contact angle decreases linearly ( $R^2=0.68$ ) with decreasing the hematite content ( $\text{Fe}_2\text{O}_{3H}$ , vol %). Thus, by combining the two points, the calculated contact angle can be obtained with the true density of the iron ores studied.

$$\theta_{cal}=29.03 \times \rho_{ore} - 93.03 (\pm 10^\circ) \quad (17)$$

Where,  $\theta_{cal}$  is the calculated contact angle based on the data of Iveson ( $^\circ$ );  $\rho_{ore}$  is the true density of the corresponding iron ore (see in Table 1).

**Table 5.** Data of the calculated contact angle based on Iveson's research

Sample	S1	S2	S3	S4	S5	S6	S7
$\theta_{cal}(\pm 10^\circ)$	32	49	51	21	25	40	37

Thus, the comparison between the measured relative contact angles ( $\theta_{RCA}$ ) in Table 3 and the calculated ones based on Iveson's data [4] can be shown in Figure 7. It shows that the calculated contact angles is in good agreement with the measured relative contact angles.

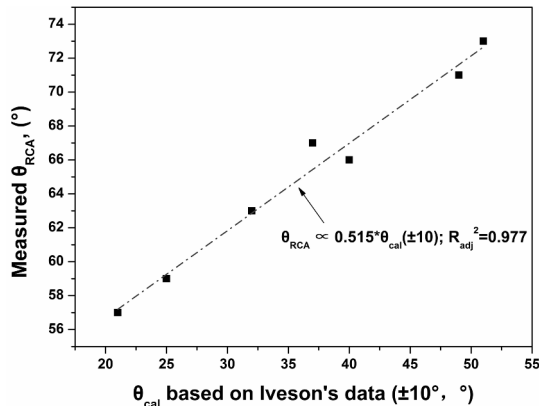


**Figure 7.** The measured  $\theta_{RCA}$  versus the calculated  $\theta_{cal}$  based on Iveson's data

However, the calculated contact angle and the measured contact angle show some difference in Figure 7. The cause of this difference can be explained with some reasons. Two possible reasons are the error in the measurement of the relative contact angle and the accumulative calculated errors of the calculated angle when applying the equations based on the data of Iveson, et al. [4]. More important, the roughness and pore structure of the iron ore particles were not taken into account in the Washburn osmotic pressure equation. It was reported by Wenzel [31], Kaptay and Barczy [33] that for hydrophilic

materials, the roughness and porous structure of the particle surfaces would lead to a better wettability of the particles with a lower contact angle. If such factors are considered in the contact angle measurement, the measured relative contact angle would decrease, more close to the calculated value.

The contact angle measured by Iveson, et al. is based on the equilibrium value of the changing pressure of the inner air, while the advancing contact angle measured in this paper is derived from the relationship between the changing pressure of the inner air and the liquid penetration time. Comparing with the research from Iveson et al. [4], a similar but more detailed conclusion was drawn in this paper that the contact angle for iron ore fines is a function of volume % of goethite and furthermore, surface morphology (SMI) and pore volume ( $V_{pore}$ ) play a role in determining the measured contact angle through the influence on the volume % of goethite.

## 5. Conclusions

With Washburn Osmotic Pressure method, the relative contact angle for seven iron ores was measured in laboratory conditions. The relative contact angle for the iron ores studied here varied from  $57^\circ$  to  $73^\circ$ . We investigated the effect of some physicochemical properties on the wettability of the iron ores. From the section of "Results and Discussion", the following conclusions can be drawn.

(1) The relative contact angle of water on iron ore fines is a function of LOI or the volume % of goethite ( $\phi_G$ ). With adhesion energy between water and goethite ( $W_G$ ) of  $0.112 \text{ J/m}^2$  and that between water and all non-hydroxide oxides ( $W_O$ ) of  $0.088 \text{ J/m}^2$ , this function can be expressed as follows.

$$\sigma_{lv} \cdot (1 + \cos(\theta)) = W_O + (W_G - W_O) \cdot \phi_G$$

Comparing with the model developed by Iveson et al., the new model proposed in this paper is similar but more detailed with two meaningful physical parameters ( $W_O$  and  $W_G$ ).

(2) Physical properties of iron ore particles, such as surface morphology (SMI) and pore volume ( $V_{pore}$ ) can influence the relative contact angle. With  $R_{adj}^2 = 0.9$  and  $SMI \geq 1$ , an empirical equation between SMI and relative contact angle ( $\theta_{RCA}$ ) was given by  $\theta_{RCA} = 90 / SMI^{0.1}$ . Given by  $\phi_G = 0.266 * SMI + 0.769 * V_{pore}$  with  $R_{adj}^2 = 0.927$ , there is a strong relation of the volume % of goethite ( $\phi_G$ ) to SMI and  $V_{pore}$ . Taking this into consideration, we can conclude that the relative contact angle is a function of the volume % of goethite ( $\phi_G$ ).

To modify physicochemical properties in order to achieve a suitable wettability between the particles and water would be another topic in the future research on wet granulation of iron ores.

### Acknowledgements

The authors are especially grateful to National Natural Science Foundation of China (NSFC) (Grant No. 51104192) for supporting and funding this work. The authors would also like to express gratitude to the reviewers from *Journal of Mining and Metallurgy, Section B: Metallurgy* for the valuable comments and suggestions on improving this paper further.

### References

- [1] S. M. Iveson, S. Holt and S. Biggs, *Colloids and Surfaces A: Physicochemical and Engineering Aspects*, 166 (1-3) (2000) 203-214.
- [2] G. Kumar and K. N. Prabhu, *Advances in colloid and interface science*, 133 (2) (2007) 61-89.
- [3] S. M. Iveson, J. A. Beath and N. W. Page, *Powder Technology*, 127 (2) (2002) 149-161.
- [4] S. M. Iveson, S. Holt and S. Biggs, *International Journal of Mineral Processing*, 74 (1-4) (2004) 281-287.
- [5] T. Maeda, C. Fukumoto, T. Matsumura, K. Nishioka and M. Shimizu, *ISIJ international*, 45 (4) (2005) 477-484.
- [6] H. Rumpf, *International Symposium on Agglomeration*, Interscience, London, UK, 1962: p. 379-419.
- [7] T. T. Chau, *Minerals Engineering*, 22 (3) (2009) 213-219.
- [8] T. H. Muster, C. A. Prestidge and R. A. Hayes, *Colloids and Surfaces A: Physicochemical and Engineering Aspects*, 176 (2-3) (2001) 253-266.
- [9] A. Siebold, M. Nardin, J. Schultz, A. Walliser and M. Oppliger, *Colloids and Surfaces A: Physicochemical and Engineering Aspects*, 161 (1) (2000) 81-87.
- [10] E. W. Washburn, *Physical review*, 17 (3) (1921) 273-283.
- [11] X. Huang and F. Gong, *Research and Exploration in Laboratory*, 22 (05) (2003) 48-50. (Chinese).
- [12] H. Luan and N. Jiao, *Journal of Lanzhou Jiaotong University*, 29 (3) (2010) 139-141. (Chinese).
- [13] Y. Thomas, *Philosophical Transactions of the Royal Society of London*, 95(1805) 65-87.
- [14] D. Y. Kwok and A. W. Neumann, *Advances in Colloid and Interface Science*, 81 (3) (1999) 167-249.
- [15] R. J. Good, *Journal of adhesion science and technology*, 6 (12) (1992) 1269-1302.
- [16] L. R. Fisher and P. D. Lark, *Journal of Colloid and Interface Science*, 69 (3) (1979) 486-492.
- [17] R. J. Good and N. J. Lin, *Journal of Colloid and Interface Science*, 54 (1) (1976) 52-58.
- [18] S. Levine, J. Lowndes, E. J. Watson and G. Neale, *Journal of Colloid and Interface Science*, 73 (1) (1980) 136-151.
- [19] J. Gaydos, *The Laplace equation of capillarity*, In *Studies in Interface Science* (edited by D. Möbius and R. Miller), Elsevier, 1998, p. 1-59.
- [20] C. E. Grosch and H. Salwen, *Journal of Fluid Mechanics*, 34 (1) (1968) 177-205.
- [21] S. M. Iveson, K. F. Rutherford and S. R. Biggs, *Transactions of the Institution of Mining and Metallurgy Section C-Mineral Processing and Extractive Metallurgy*, 110(2001) C133-C143.
- [22] L. Susana, F. Campaci and A. C. Santomaso, *Powder Technology*, 226(2012) 68-77.
- [23] L. Richard, *Colloid & Polymer Science*, 23 (1) (1918) 15-22.
- [24] D. Shen, J. Xiao and X. Chen, *SP & BMH RELATED ENGINEERING*, (1) (2007) 9-12. (Chinese).
- [25] X. Lv, X. Huang, R. Zhang and M. Zhou, *Symposium on Characterization of Minerals, Metals and Materials held during TMS Annual Meeting and Exhibition, Orlando, FL, 2012*: p. 123-129.
- [26] W. M. Haynes, *CRC handbook of chemistry and physics*, CRC press, 2012,
- [27] M. E. Schrader, *Langmuir*, 11 (9) (1995) 3585-3589.
- [28] Q. Shu, L. Wang, K.C. Chou, *J. Min. Metall. Sect. B-Metall.* 50 (2) B (2014) 139-144.
- [29] P. Baumli, J. Sytchev and G. Kaptay, *Journal of Materials Science*, 45 (19) (2010) 5177-5190.
- [30] C. Yang, F. He and P. Hao, *Science China(Chemistry)*, (04) (2010) 912-916.
- [31] R. N. Wenzel, *The Journal of Physical and Colloid Chemistry*, 53 (9) (1948) 1466-1467.
- [32] A. Marmur, *Langmuir*, 19 (20) (2003) 8343-8348.
- [33] G. Kaptay and T. Barczy, *Journal of Materials Science*, 40 (9-10) (2005) 2531-2535.